Sustainable Food Technology

ROYAL SOCIETY OF CHEMISTRY

PAPER

View Article Online
View Journal | View Issue

Cite this: *Sustainable Food Technol.*, 2024, **2**, 1569

Effect of oil–water colloidal states in liquid feeds on extrudability and textural attributes of high-moisture meat alternatives†

Florian Stehle,[b] Carlos Woern,[a] Nicholle Kirsten Tan,[a] Jochen Weiss [b] and Lutz Grossmann *[a]

The incorporation of lipids in the extrusion process to produce composite protein–lipid high-moisture meat alternatives is a major challenge due to slip conditions induced by the oil phase. This study investigates the impact of non-emulsified and emulsified liquid feeds – using soy protein isolate and *Quillaja* saponin as two different emulsifiers – at 6% oil content on the extrudability, visual appearance, textural and structural properties of a soy-based meat alternative. Homogenization pressures from 20 MPa to 140 MPa were used to achieve $d_{4,3}$ droplet sizes ranging from 1053 nm to 117 nm, respectively. The emulsions stabilized by soy protein isolate exhibited a larger droplet size at low pressures and a smaller droplet size at higher pressures compared to the emulsions containing *Quillaja* saponin (1053 nm *vs.* 659 nm at 20 MPa and 117 nm *vs.* 243 nm at 140 MPa, respectively). The addition of any kind of lipid feed resulted in a lower specific mechanical energy input compared to the standard with no oil. Non-emulsified oil reduced the directional protein fiber formation and enhanced the protein cross-linking into bulk strips, which resulted in significantly lower mechanical anisotropy compared to the standard. Emulsions stabilized by *Quillaja* saponin were able to resemble the degree of anisotropy with the smallest mean oil droplet size (243 nm) yielding a slightly higher anisotropic index than the control. Microstructural analyses revealed embedded oil droplets between protein fibers, which increased the visual fibrousness. However, only minor changes in the color measurements were observed among all treatments. The results demonstrate the potential of using emulsified liquid feeds to manufacture high-moisture meat alternatives with an incorporated oil phase by extrusion processing without losing the anisotropic character due to oil slip.

Received 4th April 2024
Accepted 14th August 2024

DOI: 10.1039/d4fb00096j

rsc.li/susfoodtech

Sustainability spotlight

Plant protein extrusion stands as a pioneering method that meets the urgent need for structuring technologies of sustainable food ingredients. This innovative process not only addresses the growing demand for plant-based protein sources but also enables the production of meat alternatives with a significantly lower ecological footprint compared to traditional livestock farming. One crucial aspect that enhances the sustainability profile of plant protein extrusion is the strategic inclusion of lipids – a key factor for consumer acceptance. The incorporation of lipids has been extremely challenging, which ultimately prevents the development of novel meat alternatives that have a higher consumer acceptance and deliver the desired flavor, texture, and nutritional properties. Understanding how lipids can be included in a continuous extrusion process will be crucial to further advance the development of meat alternatives and ultimately lower the emissions generated by the food system.

1. Introduction

The rising demand for novel plant-based fibrous foods results in (renewed) interest for novel processing solutions to deliver meat-like textures to consumers.[1,2] On the consumer side, the reasons for this interest are concerns about animal welfare as well as environmental sustainability and health concerns related to the current way the food system operates.[3–6] At present, methods to create textures that resemble the anisotropic structures of meat tissue with non-animal proteins are limited to extrusion processing, shear cell technologies, additive manufacturing, and biomanufacturing (*i.e.*, fungi cultivation).[7] Among these techniques, high moisture extrusion processing has become the most popular method to produce meat alternative products (or part of its ingredients) from plant proteins due to its flexibility, availability, and scalability.[8,9] The basic process design of this technology involves dosing a plant protein powder (concentrate or isolate) and water into the

[a]*Department of Food Science, University of Massachusetts, 100 Holdsworth Way, Amherst, MA 01003, USA. E-mail: lkgrossmann@umass.edu*

[b]*Department of Food Material Science, Institute of Food Science and Biotechnology, University of Hohenheim, 70599 Stuttgart, Germany*

† Electronic supplementary information (ESI) available. See DOI: https://doi.org/10.1039/d4fb00096j

heated barrel section (typically highest T between 130–160 °C) followed by tempering the protein melt in the cooling die where the anisotropic structure forms as a consequence of phase separation and laminar flow.[10,11]

There are, however, limitations to the extrusion process, which prevent further advancements. These include off-flavors in the final products, lack of anisotropy, high thermal load, and limited dosing capabilities for heat-sensitive ingredients as well as lipids.[12–14] Especially the absence of lipid phases in the extruded structures results in predominantly chicken-like products being released to the market. Since lipids impart several critical properties to the quality characteristics of a meat product,[15] the low-fat content of meat substitutes results in reduced juiciness and tenderness, which negatively impacts consumer acceptance.[16] The current limitation of extrusion processing to replicate the lipid phase is due to the lubricating effect of lipids which results in the slipping of the protein melt in the extrusion barrel.[17,18] Consequently, the specific mechanical energy (SME) input and wall shear stress decrease, which ultimately reduces protein polymerization and anisotropic structure formation.[13,19]

One potential approach to overcome this problem is the injection of emulsions instead of pure oil. In emulsions, the oil droplets are covered with a layer of emulsifier, which potentially could decrease the lubricity of the oil. Indeed, it was recently shown that twice the amount of oil (4% *vs.* 8%) can be injected into the barrel section when an oil-in-water emulsion stabilized by soy protein isolate is used instead of pure oil.[20] Moreover, this new method of oil addition entails the advantage of introducing fat-soluble flavor compounds or nutrients into extruded products while improving their thermal stability.[21] However, the thermal and shear stresses during the extrusion process are very high, which is why the behavior of various emulsifiers still needs to be investigated in more detail. After all, there are very limited studies assessing the concept of emulsion addition to extruded products, and the effects of different parameters on the extrudability (*i.e.*, process parameters of the extrusion process) and on the properties of the obtained composite plant protein structure (*i.e.*, textural and visual properties) are not well understood.

Hence, the present work aimed to evaluate the concept of lipid incorporation into a soy-based high-moisture extrudate through the addition of oil-in-water emulsions and its impact on the extrudability and overall properties of the meat alternative structure. To achieve a range of textures, emulsions were prepared with two different emulsifiers – soy protein isolate (SPI) and *Quillaja* saponin (QS) – at different homogenization pressures. The emulsifiers were chosen because of their compatibility with the protein matrix (SPI) and high heat stability (QS), respectively.[22] We hypothesized that smaller droplets in the feed and during the extrusion process result in improved extrudability and textural attributes.

2. Material and methods

2.1. Material

For extrusion processing, a soy protein concentrate (SPC) with a protein content of 66.1% (according to the manufacturer) was kindly donated by ADM (Decatur, IL, USA). Pure canola oil (B&G Foods Inc., Parsippany, NJ, USA) was purchased at a local supermarket and stored at 4 °C until use. The emulsifiers used for the emulsions were soy protein isolate (SPI) with a protein content of 93.1% (ADM Decatur, IL, USA) and *Quillaja* saponin (Q-Naturale 200V) with a surfactant concentration of 14% (Ingredion Incorporated Westchester, IL, USA). The oil was later dispersed in aqueous solutions of the two emulsifiers. All other chemicals used in the study were of reagent grade.

2.2. Methods

2.2.1. Emulsion preparation. To prepare the oil-in-water (O/W) emulsions, SPI and QS were solubilized in deionized water to obtain protein and surfactant concentrations of 3.0% (w/w) and 0.1% (w/w), respectively. The amount of emulsifier used was based on preliminary experiments in which these concentrations were determined for the preparation of visually stable emulsions, *i.e.*, no creaming occurred. The solutions were adjusted to pH 7 and stirred on a magnetic stirring plate at 4 °C overnight. Before emulsification, the pH was checked again and readjusted to 7. A primary emulsion was prepared using a high-shear blender (VWR 250 homogenizer, VWR International, Radnor, PA, USA) at 26 000 rpm for 2 min. To obtain different particle sizes, the primary emulsions were homogenized at 20, 50, 90, and 140 MPa for 3 cycles in two different high-pressure homogenizers with different pressure ratings (APV 1000, APV Homogenizers AS, Albertlund, Denmark, and M-110P, Microfluidics Corporation, Newton, MA, USA). Emulsions were formulated with an oil content of 9.6% (w/w), which resulted in a final oil content of 6% (w/w) in the high-moisture meat alternatives (HMMA) after the extrusion process (Table 1). The emulsions were used for the extrusion process on the same day.

2.2.2. Emulsion characterization. The effect of homogenization pressure and type of surfactant was determined by measuring the droplet size distribution of the emulsions using a laser diffractometer (Mastersizer 3000, Malvern Instruments Ltd, Worcester, UK; refractive index: 1.465). The results are reported as volume-based frequency distributions based on the Mie theory and the $d_{4,3}$ droplet mean size was computed by the device according to eqn (1).

$$d_{4,3} = \frac{\sum d^4}{\sum d^3} \quad (1)$$

Further, the rheological properties of the emulsions were evaluated by measuring the viscosity using a stress-controlled rheometer (MCR 302e, Anton Paar, Graz, Austria) equipped with a double gap geometry. The shear rate was increased from 10 to 100 s^{-1} at constant temperature of 25 °C and the apparent viscosity was calculated from the slope of the shear stress *vs.* shear rate diagram.

2.2.3. Extrusion process. The extrusion was performed on a co-rotating, intermeshing twin-screw extruder (ZE 12 HMI, Three-Tec GmbH, Seon, Switzerland) with a screw diameter of 12 mm and a length-to-diameter ratio of 40. The barrel consisted of 7 individually heated sections, with the first section consistently water-cooled at 10 °C to prevent baking of the

Table 1 Composition of the emulsions and soy-based extrudates prepared with no oil (standard), non-emulsified oil (control), non-emulsified oil plus soy protein isolate (control + SPI) or *Quillaja* saponin (control + QS), and oil emulsions stabilized by soy protein isolate (SPI) or *Quillaja* saponin (QS). The SPI or QS was dissolved in the water to reach final concentrations of 3.0% and 0.1%, respectively[a]

	Emulsion (%)		Extrudate (%)		
Sample	Water/surfactant solution	Oil	Water/surfactant solution	Oil	SPC
No oil					
Standard	—	—	60	—	40
Non-emulsified oil					
Control	100	—	57	6	37
Control + SPI/QS	100	—	57	6	37
Emulsified oil					
SPI/QS	90.4	9.6	57	6	37

[a] The symbol (—) denotes for the component being not present in the emulsion/extrudate.

protein powder feed to the inlet section. A temperature ramp of 80, 100, 100, 120, 140 and 160 °C was operated for the remaining barrel sections. Approximately the first 30% of the total screw length consisted of fixed forward conveying elements with a pitch of 12 mm and a higher conveying volume to facilitate the powder feed. The remaining screw configuration was set as follows: 3 forward conveying elements (12 mm pitch), 1 mixing/reverse conveying element (12 mm pitch), 4 forward conveying elements (12 mm pitch), 2 kneading elements (60 and 90°), 7 forward conveying elements (12 mm pitch), 1 forward conveying element (9 mm pitch) and 1 forward conveying element (12 mm pitch) – each element had a length of 18 mm (Fig. 1). A conical flange with a plate insert containing 13 holes of 3.2 mm in diameter – so called "breaker plate" – attached a cooling die (length: 300 mm; width: 15 mm; height: 4 mm) to the end section of the barrel. To allow for proper texturization, the cooling die was temperature-controlled by a 1740 W recirculating chiller (DuraChill®, VWR, Radnor, PA, USA) at 40 °C. The total throughput was set to 1 kg h^{-1} at a screw speed of 300 rpm and the process was allowed to stabilize for at least 5 min before samples were taken.

Table 1 shows the four different extrudate formulations: (1) *Standard*: SPC and water with no oil feed; (2) *Control*: SPC and water with non-emulsified oil feed; (3) *Control + Emulsifier*: Composition similar to (2) plus emulsifier (SPI or QS) solubilized in the water feed; (4) *Emulsified treatments*: SPC and emulsion feed. The SPC powder was fed into the first barrel section using a volumetric screw feeder (ZD 9 FB-C-1M-DN80, Three-Tec GmbH, Seon, Switzerland). The water and emulsion feed, respectively, were injected through a liquid port into the second barrel section using a peristaltic pump (Three-Tec GmbH, Seon, Switzerland). For processing formulations (2) and (3), the non-emulsified oil feed was pumped into the third barrel section using a high-pressure piston pump (AZURA P 4.1S, KNAUER Wissenschaftliche Geräte GmbH, Germany).

All treatments were formulated to achieve a consistent water-to-protein ratio of 1.5 (Fig. 1) and thereby a proper protein hydration was ensured, also for formulations in which a portion of the water phase was replaced with oil. Consequently, the standard treatment comprised 40% (w/w) SPC and 60% (w/w) water, while the remaining treatments contained 37% (w/w)

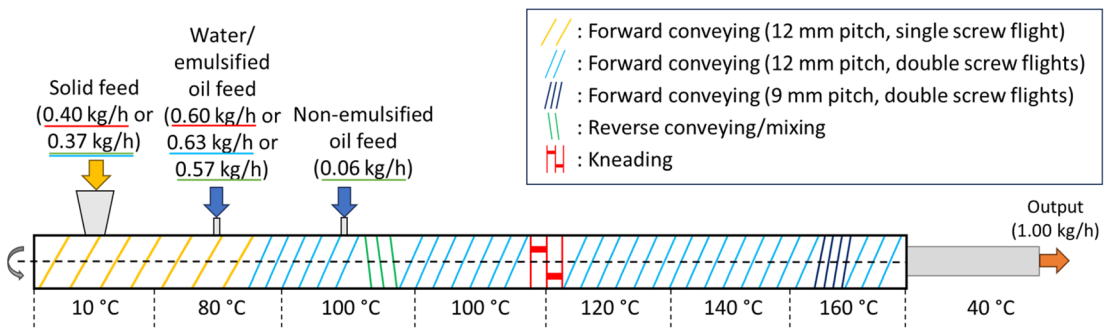

Fig. 1 Extruder design and operating parameters for the extrusion process of composite high moisture meat alternatives. The feeding rates operated for the standard are underlined in red, the feeding rates for the emulsified oil samples are underlined in blue and the feeding rates for the non-emulsified oil samples are underlined in green.

SPC, 57% (w/w) aqueous SPI or QS solution, and 6% (w/w) canola oil (Table 1). Finally, the extruded HMMA samples were cooled to room temperature, packed in sealed plastic bags, and stored at 4 °C until further analysis.

2.2.4. Extrudability. The process characterizing parameters were documented to evaluate the extrudability of the different treatments. Therefore, the temperature profile for each barrel section (2 to 7) and the cooling die, the pressure at the end of the last barrel section (7, see Fig. 1), and the torque together with the rotational speed of the screw were monitored and recorded every second. Representative values for the die pressure and screw torque were obtained by averaging all measured values over the time period in which samples were taken. The SME was calculated using eqn (2):[23]

$$\mathrm{SME} = \frac{P}{\dot{m}} = \frac{\omega M}{\dot{m}} = \frac{2\pi n M}{\dot{m}} \quad (2)$$

Here, P is the motor power in kJ s^{-1}, $\dot{m}$ is the total throughput in kg min^{-1}, ω is the angular velocity in s^{-1}, M is the screw torque in N m, n is the screw rotation speed in rpm.

2.2.5. Texture analysis. To determine the textural properties of the HMMA treatments, a tensile test was performed using a texture analyzer (TA-XT-PLUS, Stable Micro Systems Ltd, Surrey, UK) equipped with a 5 kg load cell and serrated tensile grips (TA-96BW). The distance between the bottom and top grip was set to 4 mm at the starting position and the strain rate was 0.1 mm s^{-1}. 10 samples were tested for both parallel and perpendicular to the fiber direction and cut to a length of 50 mm and 30 mm, respectively.

As a parameter quantifying the deformation behavior, the maximum stress was identified for each treatment and the corresponding anisotropy index (AI_σ) was calculated using eqn (3).[24]

$$\mathrm{AI}_\sigma = \frac{\sigma_{\mathrm{para}}}{\sigma_{\mathrm{perp}}} \quad (3)$$

where σ_{para} is the maximum stress recorded for tension exerted parallel to the fiber direction and σ_{perp} is the maximum stress for tension exerted perpendicular to the fiber direction.

From the linear (elastic) deformation, the Young's modulus (E) was calculated based on eqn (4) as a measure for the stiffness of the material. Further, the elastic anisotropy index (AI_E) was defined as the ratio between the parallel and perpendicular Youngs's modulus (eqn (5)):[25]

$$E = \frac{\Delta\sigma}{\Delta\gamma} \quad (4)$$

$$\mathrm{AI}_\mathrm{E} = \frac{E_{\mathrm{para}}}{E_{\mathrm{perp}}} \quad (5)$$

$\Delta\sigma$ is the change in tensile stress within the linear region, $\Delta\gamma$ is the change in tensile strain within the linear region, E_{para} is the Young's modulus determined for deformation parallel to the fiber direction, and E_{perp} is the Young's modulus determined for deformation perpendicular to the fiber direction.

2.2.6. Microstructure and visual appearance. The microstructure of the samples was revealed using a confocal laser scanning microscope (Nikon D-Eclipse C2+, Nikon, Melville, NY, USA). The samples were put in the freezer for 1 h at −20 °C and thinly sliced to ensure optimal resolution quality. The protein phase was stained with 0.5 mg mL^{-1} fluorescein isothiocyanate and the oil phase was stained with 0.5 mg mL^{-1} Nile red (Sigma-Aldrich, St. Louis, MO, USA) dissolved in 95% ethanol (Fisher Science Education, Nazareth, PA, USA). Images were captured using a 20× objective lens with excitation wavelengths of 488 and 561 nm and analyzed using an image analysis software (NIS-Elements, Nikon, Melville, NY, USA).

Photos of the surface and inside – torn in parallel and perpendicular direction to the fiber formation – were taken to compare the visual appearance and fibrousness of all treatments.

2.2.7. Color evaluation. The surface color of 12 samples from each HMMA treatment was determined with a colorimeter (ColorFlex EZ 45/0-LAV, HunterLab, Reston, Virginia, USA) using a D65 illuminant and 10° standard observer. Values were expressed according to the Commission Intl. de l'Eclairage (CIE) system and reported as L^* (lightness), a^* (redness) and b^* (yellowness) values.[26] Additionally, color difference (ΔE^*) was calculated using the Euclidean distance to quantify the interactions of the color parameters.[27]

2.2.8. Statistical analysis. The experiment was designed with 2 separate replications. Statistical analysis was performed using SPSS statistics V25 (IBM Corp., Armonk, NY, USA). A one-way ANOVA with a Duncan *post hoc* test was carried out to evaluate statistically significant differences (α-level of 0.05). Data was graphed using Origin Pro (OriginLab Corp., Northampton, MA, USA) with error bars indicating the standard deviation.

3. Results and discussion

3.1. Effect of homogenization pressure and surfactant properties on emulsion characteristics

The experiment involved two emulsifiers that are commonly used in the production of composite foods but rely on different properties to control the interfacial behavior. SPI is a large biopolymer with a high compatibility for incorporation into a protein-based matrix, whereas QS is a small and heat-stable amphiphilic molecule. These properties might also have a substantial impact on the processing, texture, and visual appearance of soy-based HMMA. Therefore, the emulsifying efficacy under high pressure homogenization of both surfactants was evaluated to understand the potential effect on the properties of HMMA samples.

It is well known that the applied pressure is inversely correlated with the droplet size.[28] As expected, the droplet size decreased with higher homogenization pressures for both emulsifiers (Fig. 2). At a low homogenization pressure of 20 MPa, the SPI-stabilized emulsion exhibited a larger droplet size than the QS-stabilized emulsion (1053 nm *vs.* 659 nm). However, this trend was reversed for homogenization at 90 MPa and 140 MPa, as the oil droplets in the QS-stabilized emulsions were significantly larger (279 and 243 nm) compared to the SPI-stabilized emulsions (155 and 117 nm) (Table 2). Low-molecular

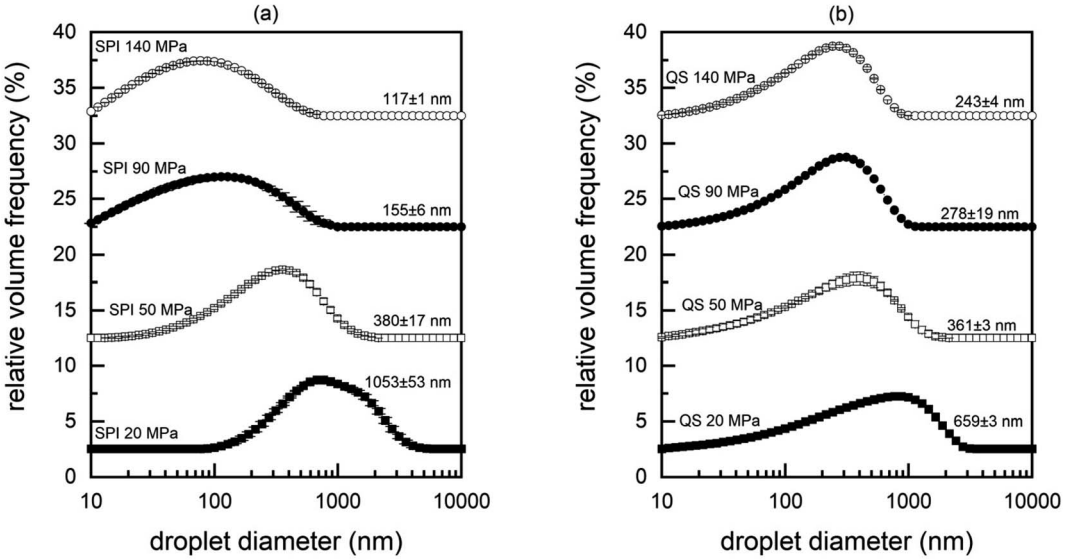

Fig. 2 Volume-based particle size distribution and the corresponding mean particle size $d_{4,3}$ of emulsions homogenized at four different pressures (20, 50, 90 & 140 MPa) and stabilized by soy protein isolate (SPI) addition (a) and *Quillaja* saponin (QS) addition (b), respectively.

weight emulsifiers tend to adsorb faster to interfaces and lower the interfacial tension faster than high-molecular weight emulsifiers.[28] The faster adsorption results in more efficient droplet disruption and stabilization in QS-stabilized emulsions already at lower pressures. In particular, QS has been shown to be a very efficient emulsifier compared to larger biopolymer emulsifiers.[22] Still, the chosen QS concentration of 0.1% may not have been sufficient to fully adsorb and cover the generated oil–water interface at higher pressures, resulting in larger droplet sizes compared to SPI-stabilized emulsions.

Table 2 Effects of homogenization pressure and corresponding volume-based mean particle size ($d_{4,3}$) on the extrudability of soy-based extrudates prepared with no oil (standard), non-emulsified oil (control), non-emulsified oil plus soy protein isolate (control + SPI) or *Quillaja* saponin (control + QS), and oil emulsions stabilized by soy protein isolate (SPI) or *Quillaja* saponin (QS). Oil concentration in the final extrudate was at 6%[a]

Treatment	$d_{4,3}$ (nm)	Die pressure (MPa)	SME (kJ kg^{-1})
No oil			
Standard	—	1.33 ± 0.01^{b}	326 ± 8^{d}
Non-emulsified oil			
Control	—	1.22 ± 0.08^{ab}	293 ± 16^{c}
Control + SPI	—	1.25 ± 0.06^{ab}	278 ± 15^{abc}
Control + QS	—	1.23 ± 0.05^{ab}	266 ± 15^{ab}
Emulsified oil			
SPI 20 MPa	1053 ± 53^{e}	1.15 ± 0.08^{a}	293 ± 19^{c}
SPI 50 MPa	380 ± 17^{c}	1.19 ± 0.09^{ab}	288 ± 8^{bc}
SPI 90 MPa	155 ± 6^{a}	1.26 ± 0.02^{ab}	279 ± 3^{abc}
SPI 140 MPa	117 ± 1^{a}	1.19 ± 0.02^{ab}	294 ± 18^{c}
QS 20 MPa	659 ± 3^{d}	1.24 ± 0.05^{ab}	267 ± 5^{ab}
QS 50 MPa	361 ± 3^{c}	1.15 ± 0.18^{a}	268 ± 11^{abc}
QS 90 MPa	278 ± 19^{b}	1.29 ± 0.06^{ab}	258 ± 7^{a}
QS 140 MPa	243 ± 4^{b}	1.33 ± 0.02^{b}	259 ± 5^{a}

[a] [a–e]Means ($n = 2$) ± standard deviation, within a column followed by different superscripts are significantly different ($P < 0.05$). For volume-based mean particle size ($d_{4,3}$), the symbol (—) denotes for no observations as no homogenization was performed for these treatments.

To further characterize and understand the flow behavior of the emulsions, the viscosity was analyzed (see ESI†). Interestingly, the droplet size had no effect on the measured viscosity. In such diluted emulsion systems, the viscosity is mainly influenced by the viscosity of the continuous phase, and thus the particle size had no significant impact on the measurements.[29] The viscosity of the QS-stabilized emulsions was 1.41 ± 0.09 mPa s at all shear rates, *i.e.*, higher than that of pure water (around 1 mPa s). In contrast, the SPI-stabilized emulsions showed shear thinning behavior, but no correlation between viscosity and droplet size was found. Nevertheless, these differences may have important implications for the extrusion process. The high shear conditions in the extruder – which can reach several hundred s^{-1} – can affect the viscosity of shear-thinning materials.[30] Low viscosities, in turn, reduce the SME and can decrease the degree of protein polymerization in the extruder, which changes the textural properties of the HMMA.[31]

3.2. Emulsion colloidal state and its effect on extrudability of composite HMMA

To compare the effects of lipid phase injection (non-emulsified and emulsified) during the extrusion process of HMMA production, the die pressure, screw speed, and torque were recorded and averaged for each sample. The screw speed and torque were used to calculate the SME using eqn (2).[23]

The addition of non-emulsified oil to the barrel section of the extrusion process did not have a significant effect on the die

pressure compared to the standard with no oil addition (Table 2). Here, the lubricating effect of an oil feed in the extrusion process did not result in a reduced die pressure, which is in contrast to reported literature.[17,18] Presumably, the oil was sufficiently incorporated into the matrix so that no film formed on the barrel surface. On the other hand, the SME showed a significant decrease for treatments with bulk oil addition compared to the standard. This effect was pronounced for the non-emulsified control plus QS (Table 2). The SME reflects the required energy input based on material resistance and process conditions, and is therefore influenced by material properties such as degree of polymerization and viscosity. In the controls with emulsifiers added to the water feed, less energy was required to transport and knead the matrix in the barrel. Emulsifiers, particularly QS, are known to efficiently reduce the interfacial tension which promotes the spreading and wettability of surfaces by increasing the surface energy.[32] Therefore, the emulsifiers most likely facilitated the spreading of the bulk oil in the barrel during the conveying and kneading, which promoted the wetting of the inner barrel surface and consequently decreased the SME. The fact that there was no significant difference between the control without emulsifier and the control with SPI addition could be attributed to the fact that SPI does not inhibit the cross-linking and, unlike QS, can be incorporated into the network. Due to their chemical structure, proteins form covalent and non-covalent bonds which determines the texture of the extrudates.[33] The chemical structure of the small saponin molecules differs fundamentally from that of proteins.[34] The saponins might interact with the protein phase and negatively affect their crosslinking,[35] but more studies are needed to confirm this.

In contrast to the non-emulsified oil samples, the SPI 20 MPa and QS 50 MPa treatments resulted in significantly lower die pressures (1.15 MPa for both treatments) compared to the standard without oil (1.33 MPa; Table 2). For the SPI 20 MPa treatment, the reduction in die pressure might be related to the large droplet size in the emulsion. Kendler *et al.*[13] found that adding oil at an earlier point of the barrel reduced the die pressure compared to a point closer to the extrusion die. However, the distance between the two addition points reported in this study was greater than in our experimental setup. If the emulsion has similar properties like the bulk oil due to large droplets, further investigation is needed to prove the influence of the slightly earlier addition point in our case. The other emulsion treatments did not show a significant difference in die pressure to either the standard or the non-emulsified controls. This might be related to the fact that the die is relatively large (cross-sectional area) and the breaker plate has 13 holes with a diameter of 3.2 mm. Therefore, the build-up of a high back pressure is not likely and the effect of a change in composition might be negligible.

Interestingly, the SME showed the opposite trend. All treatments with emulsified oil resulted in significantly lower SME values compared to the standard. However, the SPI-stabilized emulsion treatments showed no significant difference to the respective control treatments, while most QS-stabilized emulsion treatments had a significantly lower SME input compared to the non-emulsified control without emulsifier addition (Table 2). This is most likely a direct result of reduced interfibrillar protein cross-linking caused by the embedment of the small QS-stabilized oil droplets within the fiber network. Only a slight, non-significant reduction in SME was seen for the SPI-stabilized emulsion which means the SPI most likely desorbs from the oil interface and gets incorporated into the protein network. This supports protein network formation, which may accelerate or enhance matrix polymerization and increases the SME by increasing the melt viscosity compared to QS-stabilized samples and counteracts the slipping induced by the oil phase.[31]

3.3. Deformation behavior and mechanical anisotropy in composite HMMA

To evaluate the mechanical properties of the HMMA, a tensile test was performed exerting tension parallel and perpendicular to the fiber direction of the samples. Fig. 3 shows the maximum tensile stress in parallel (σ_{para}) and perpendicular direction (σ_{perp}) as well as the calculated tensile stress anisotropy index (AI_σ) for treatments formulated with emulsions stabilized by SPI and QS, respectively, compared to the standard without oil and the respective non-emulsified controls with added oil.

Among the SPI treatments, no significant differences in maximum tensile stress were observed for both parallel and perpendicular testing (Fig. 3A). Still, the highest values for σ_{para} (371 kPa) and σ_{perp} (261 kPa) were obtained for the control with SPI addition. Here, the oil phase might have facilitated and assisted in the phase separation, while the SPI was easily incorporated into the continuous protein matrix. Both effects led to the formation of a stronger and more pronounced protein network reflected in the higher values. Still, no increase in the degree of anisotropy was observed as higher values were measured for both parallel and perpendicular testing, but rather a slight drop in AI_σ compared to the standard. Interestingly, the SPI-stabilized emulsified feed also did not show a significant increase in stress-based AI_σ even though the particle size obtained in the emulsion was smaller compared to the QS-stabilized emulsions. However, SPI-stabilized emulsions are also less heat stable compared to QS-stabilized emulsions and start to break down at elevated protein concentrations at around 75 °C,[22,36] which probably led to emulsion breakdown in the barrel section of the extruder at higher temperatures. In addition, the remaining droplets can crosslink the individual fibers because the interface is coated with SPI, which can induce protein–protein crosslinks (Fig. 4a). This resulted in a significantly lower value for the SPI 50 MPa treatment compared to the standard with no oil (Fig. 3A).

Emulsified treatments using QS also showed no significant differences in σ_{para} values (Fig. 3B), but in contrast to SPI-stabilized treatments, a clear trend in σ_{perp} values was observed, *i.e.*, the higher the homogenization pressure the lower the maximum tensile stress for perpendicular tension (Fig. 3B). The perpendicular tensile strength of the QS 140 MPa treatment (111 kPa) substantially declined by almost 50% compared to the non-emulsified control without emulsifier

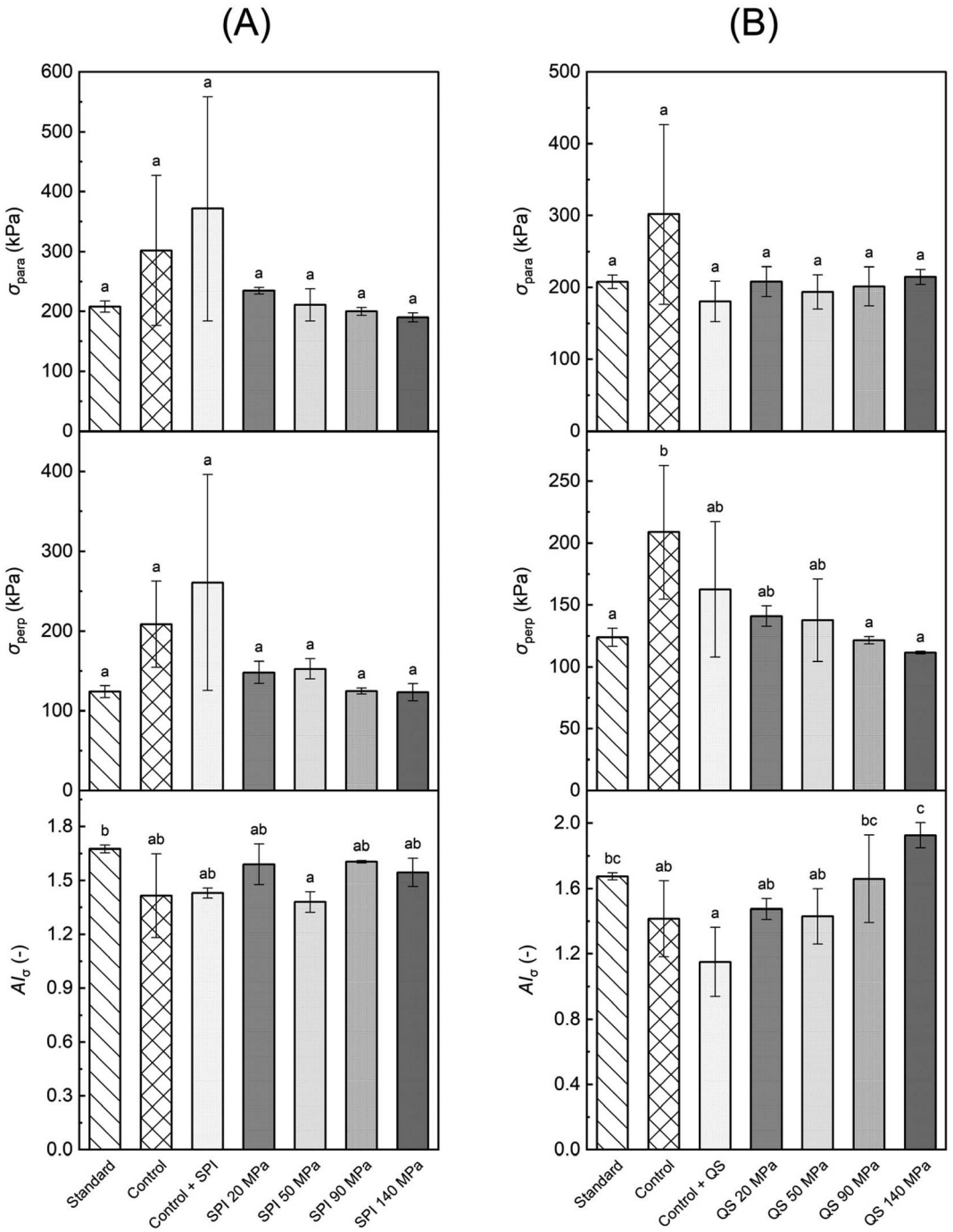

Fig. 3 Maximum tensile stress in parallel (σ_{para}) and perpendicular direction (σ_{perp}) to the fiber orientation as well as the calculated stress-based anisotropy index (AI_σ) of soy protein-based high-moisture meat alternatives prepared with no oil (standard), non-emulsified oil (control), non-emulsified oil plus soy protein isolate (control + SPI) or *Quillaja* saponin (control + QS), and oil-in-water emulsions homogenized at 20, 50, 90, or 140 MPa and stabilized by the addition of SPI (A) or QS (B). Error bars indicate the standard deviation ($n = 2$). $^{a-c}$Bars with different superscripts are significantly different ($P < 0.05$).

addition (209 kPa). Here, the emulsified oil droplets were able to separate the individual fibers and thereby reduce the interfibrillar cross-linking (Fig. 4b). This trend further affected the AI_σ values with higher indices the higher the homogenization pressure (Fig. 3B). The significantly lowest AI_σ was revealed by the non-emulsified control with QS addition. This is related to the relatively low tensile strength of the HMMA in the parallel direction. As described in the previous paragraph, the non-emulsified bulk oil amplifies the phase separation which strengthened the protein network but not necessarily promoted the directional protein fiber formation expanding into a single spatial dimension, *i.e.*, the definition of mechanical

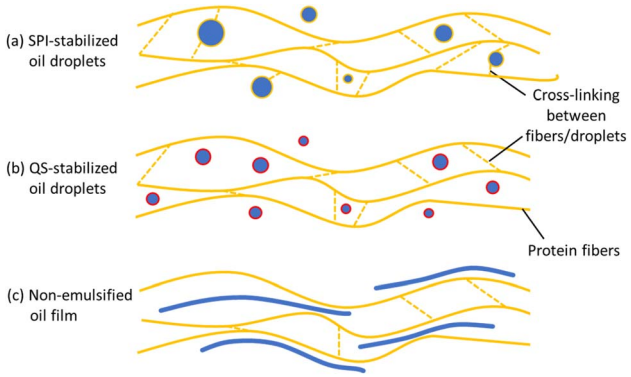

Fig. 4 Schematic illustration depicting the microstructure and oil droplet embedding into the continuous protein matrix of high-moisture meat alternatives prepared with a soy protein isolate (SPI) stabilized emulsion feed (a); prepared with a *Quillaja* saponin (QS) stabilized emulsion feed (b); prepared with a non-emulsified oil feed (c).

anisotropy.[14] Moreover, the oil in combination with the QS accelerated the wetting and lubrication of the protein layers, which reduced the force required to pull the protein fibers in the parallel direction and reduced the tensile strength in the parallel direction, but to a lesser extent in perpendicular direction.

To get a more comprehensive understanding of the texture formation in the HMMA treatments, the mechanical properties under elastic deformation were analyzed. In contrast to the analysis at maximum tensile strength right before the texture fractures, the protein fibers are still intact within the linear region of the stress–strain diagram and are only elastically stretched.

A remarkable trend in the parallel (E_{para}) and perpendicular Young's modulus (E_{perp}) was observed for the SPI-stabilized (Fig. 5A) as well as for the QS-stabilized treatments (Fig. 5B): the addition of non-emulsified oil resulted in the lowest values, while the emulsified treatments were able to resemble the standard with no oil. A higher Young's modulus has been previously correlated with a higher degree of fibrousness in HMMA,[13,37] which means that the incorporation of non-emulsified oil resulted in a pronounced and softer protein network – due to the phenomena stated above – but less directional protein structure formation (Fig. 4c). On the other hand, introducing emulsified oil into the extrusion process yielded stiffer and more fibrous HMMA samples. However, these findings were only substantiated by the elastic anisotropy indices (AI_E) of the treatments including QS. Here, the treatments with the highest homogenization pressures of 90 MPa and 140 MPa resulted in significantly higher AI_E values (1.25 & 1.31) compared to the non-emulsified oil treatment plus QS (0.82) (Fig. 5B). No significant differences in the AI_E values were seen for SPI-stabilized treatments (Fig. 5B). This might be associated with a stronger interfibrillar cross-linking induced by the SPI and therefore attenuating the direction-dependance of the deformation behavior (Fig. 4A).

3.4. Morphology of the oil phase and its impact on the visual appearance of composite HMMA

The identification of possible differences at the microstructural level between all treatments was achieved through visualization *via* CLSM imaging. For the non-emulsified controls, all images revealed an oil film that was spread throughout the samples with some visible isolated patches embedded between the protein networks (Fig. 6). This supports the conclusions drawn from the texture analysis that bulk oil intensifies the phase separation and leads to the formation of more pronounced protein segments within the HMMA. On the other hand, CLSM analysis of the emulsified treatments showed visible intact oil droplets dispersed within the surrounding continuous protein network. Regardless of the emulsifier used, the incorporated oil droplets were bigger than expected and substantially larger than the droplets in the initial emulsion (Fig. 2). Most of the droplets embedded in the HMMA were in the size range of a few μm (5–10 μm) with clear signs of coalescence. It can be assumed that the emulsions were destabilized by the extrusion process and the fat droplets coalesced due to the high temperature.[38] In the case of SPI, this is favored by the denaturation of the protein, which changes the conformation and thus also the emulsifying properties.[39] Further, the SPI might have been incorporated into the protein network and thus cannot act as an emulsifier anymore. The remaining amount of SPI is no longer sufficient to stabilize smaller oil droplets. QS, on the other hand, is not affected by the high temperature during extrusion.[22,40,41] The smaller droplet size in the samples with QS-stabilized emulsions compared to the ones with SPI may be related to the fast adsorption rate of QS to the interface, which stabilizes the coalesced droplets again when being sheared in the extruder.[42] Reichert *et al.*[43] also reported that interfaces consisting of QS showed a higher viscoelastic stability than interfaces consisting of pea protein. It can therefore be assumed that the QS-stabilized droplets are less affected by shearing in the extruder than the SPI-stabilized droplets due to their mechanical stability. Consequently, the smaller droplets in the emulsified QS samples might be responsible for the enhanced directional protein fiber formation and prevent the interfibrillar protein cross-linking, which resulted in a higher mechanical anisotropy index – elastic and stress-based – compared to the non-emulsified controls (see Section 3.3).

Visual macroscale fibrous structures were formed for all non-emulsified oil samples, with the fibrousness appearing higher compared to the standard without oil (Fig. 7b and c). It must be pointed out that the visual assessment of fibrousness is only useful in direct and descriptive comparison of the samples and can hardly be used as a standardized method.[44] The presence of oil might enhance the formation of visual fibers by preventing the cross-linking of larger protein strings after separation in the breaker plate, which fosters the visual appearance of fibrousness. As hierarchy and compartmentation play a crucial role in the anisotropic properties of HMMA,[14] this visual fibrousness is not reflected in the measured mechanical anisotropy of the non-emulsified treatments because of the more pronounced

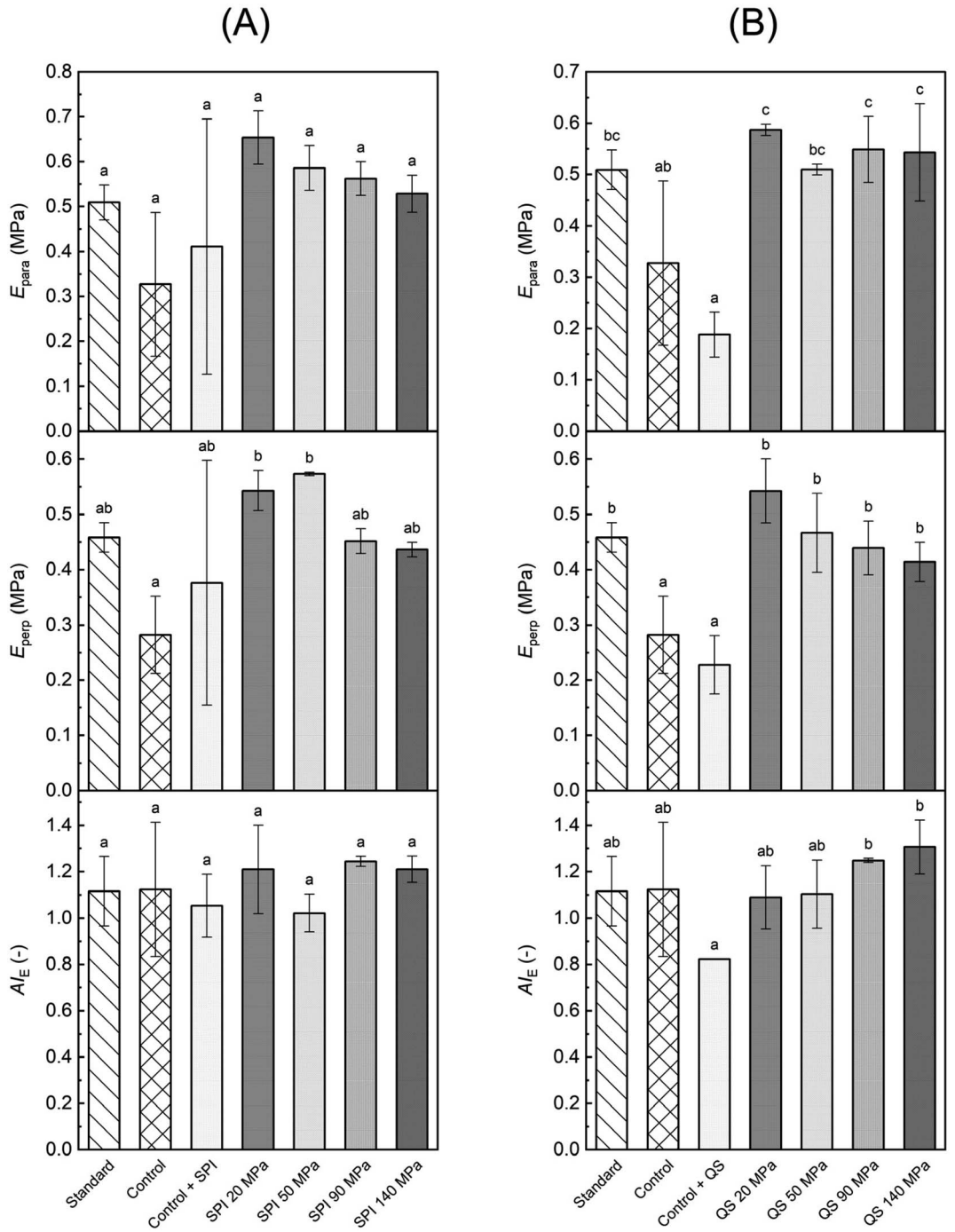

Fig. 5 Young's moduli with tension exerted in parallel (E_{para}) and perpendicular direction (E_{perp}) to the fiber orientation as well as the calculated elastic anisotropy index (AI_E) of soy protein-based high-moisture meat alternatives prepared with no oil (standard), non-emulsified oil (control), non-emulsified oil plus soy protein isolate (control + SPI) or *Quillaja* saponin (control + QS), and oil-in-water emulsions homogenized at 20, 50, 90, or 140 MPa and stabilized by the addition of SPI (A) or QS (B). Error bars indicate the standard deviation ($n = 2$). $^{a-c}$Bars with different superscripts are significantly different ($P < 0.05$).

reduction in tensile stress in the parallel direction (Fig. 3A), which results in a more isotropic substructure, *i.e.*, non-directional protein cross-linking. Such phenomena have also been observed by other authors, who reported extensive visual fibrousness that was not reflected in tensile test measurements.[45] Similarly, all the emulsified treatments exhibited a higher visual fibrousness compared to the standard, but on a visibly smaller length scale than the non-emulsified controls (Fig. 7b and c). The addition of emulsions may have promoted anisotropic structure formation through an induced spatial separation that prevents cross-linking between individual protein fibers based on the reduction of extensive non-directional intermolecular polymerization and protein–protein interaction.[14] However, the HMMAs with injected emulsions all

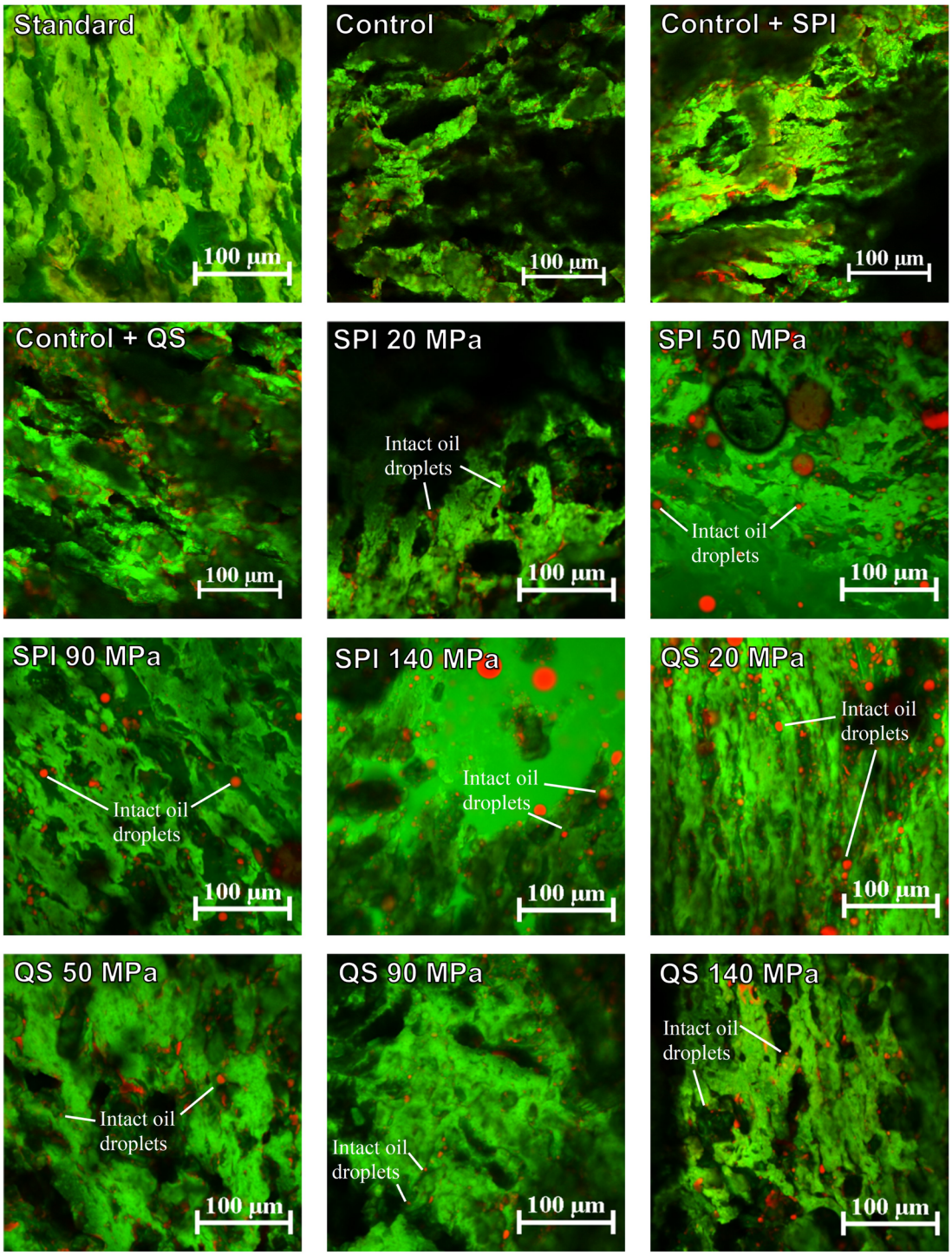

Fig. 6 Microstructure of the high-moisture meat alternatives prepared with no oil (standard), non-emulsified oil (control), non-emulsified oil plus soy protein isolate (control + SPI) or *Quillaja* saponin (control + QS), and oil-in-water emulsions homogenized at 20, 50, 90, or 140 MPa and stabilized by the addition of SPI or QS. Structures were visualized through confocal laser scanning microscopy (CLSM) with the oil phase stained red and the protein matrix stained green. Samples were cut perpendicular to the fiber direction.

showed a slight oil film on the surface, so it can be assumed that the emulsion was destabilized during the extrusion process (Fig. 7a). Such effects have also been observed by other authors, who reported extensive visual anisotropy that was not reflected in tensile test measurements.[45]

3.5. Color evaluation

The addition of non-emulsified bulk oil resulted in higher L^*-, lower a^*-, and lower b^*-values compared to the standard without oil (Table 3). However, only the control with QS showed significant differences to the standard for all three parameters,

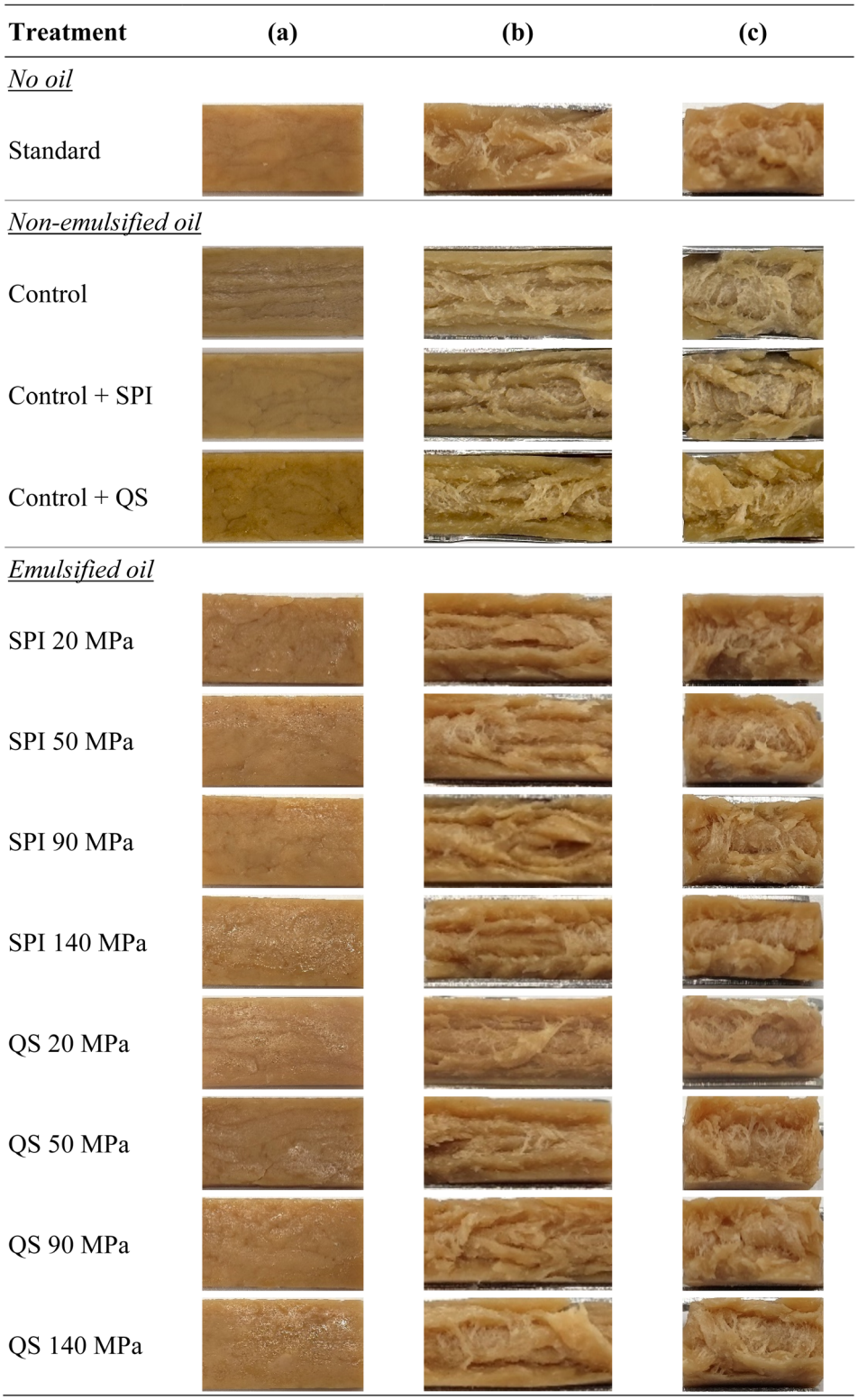

Fig. 7 Images of high-moisture meat alternatives prepared with no oil (standard), non-emulsified oil (control), non-emulsified oil plus soy protein isolate (control + SPI) or *Quillaja* saponin (control + QS), and oil-in-water emulsions homogenized at 20, 50, 90, or 140 MPa and stabilized by the addition of soy protein isolate (SPI) or *Quillaja* saponin (QS). Effect on visual fibrousness of the surface (a) and inside when torn parallel (b) or perpendicular (c) to the fiber orientation.

while for the control and the control with SPI only differences in the a^*-value and b^*-value were of significance, respectively. The uniqueness of the control with QS might be related to the good emulsifying ability of saponins due to their small molecule size, which favors the formation of small droplets and, consequently, light scattering. This increases the brightness of the samples

Table 3 Effects of homogenization pressure and corresponding volume-based mean particle size ($d_{4,3}$) on surface color (L^* = lightness, a^* = redness, b^* = yellowness, $\Delta E_{standard}$ = color difference to standard, $\Delta E_{control}$ = color difference to control, $\Delta E_{control\ emul}$ = color difference to control plus respective surfactant) of soy-based extrudates prepared with no oil (standard), non-emulsified oil (control), non-emulsified oil plus soy protein isolate (control + SPI) or *Quillaja* saponin (control + QS), and oil emulsions stabilized by soy protein isolate (SPI) or *Quillaja* saponin (QS). Oil concentration in the final extrudate was at 6%[a]

Treatment	$d_{4,3}$ (nm)	L^*	a^*	b^*	$\Delta E_{standard}$	$\Delta E_{control}$	$\Delta E_{control\ emul}$
No oil							
Standard	—	30.8 ± 0.6^{a}	10.8 ± 0.8^{b}	19.7 ± 0.9^{d}	—	2.6	2.3 (SPI)/5.8 (QS)
Non-emulsified oil							
Control	—	33.3 ± 1.3^{cd}	10.7 ± 0.5^{b}	19.0 ± 0.6^{cd}	2.6	—	1.5 (SPI)/4.0 (QS)
Control + SPI	—	32.2 ± 0.1^{abc}	10.3 ± 0.4^{b}	18.0 ± 0.9^{bc}	2.3	1.5	—
Control + QS	—	34.5 ± 0.7^{d}	9.2 ± 0.4^{a}	15.5 ± 0.8^{a}	5.8	4.0	—
Emulsified oil							
SPI 20 MPa	1053 ± 53^{e}	32.8 ± 0.8^{abcd}	8.9 ± 0.4^{a}	18.1 ± 1.1^{b}	3.2	2.1	1.5
SPI 50 MPa	380 ± 17^{c}	31.9 ± 0.1^{abc}	9.1 ± 0.4^{a}	18.8 ± 0.9^{bcd}	2.2	2.1	1.4
SPI 90 MPa	155 ± 6^{a}	32.3 ± 1.7^{abc}	9.0 ± 0.4^{a}	18.4 ± 0.4^{bcd}	2.8	2.0	1.4
SPI 140 MPa	117 ± 1^{a}	32.7 ± 0.2^{abcd}	8.7 ± 0.2^{a}	18.0 ± 0.7^{bc}	3.3	2.3	1.7
QS 20 MPa	659 ± 3^{d}	31.9 ± 0.5^{abc}	8.8 ± 0.1^{a}	17.8 ± 0.0^{bc}	3.0	2.6	3.5
QS 50 MPa	361 ± 3^{c}	32.9 ± 0.3^{bcd}	8.5 ± 0.1^{a}	17.3 ± 0.2^{b}	3.9	2.8	2.5
QS 90 MPa	278 ± 19^{b}	31.1 ± 1.1^{ab}	8.9 ± 0.1^{a}	17.9 ± 0.2^{bc}	2.7	3.0	4.1
QS 140 MPa	243 ± 4^{b}	31.2 ± 1.2^{ab}	8.9 ± 0.2^{a}	18.5 ± 0.3^{bcd}	2.3	2.8	4.4

[a] [a–e]Means ($n = 2$) ± standard deviation, within a column followed by different superscripts are significantly different ($P < 0.05$). The symbol (—) denotes for no data available.

and promotes a whiter appearance. Surprisingly, the QS-stabilized emulsified treatments resulted in lower L^* values, *i.e.* a darker surface, compared to the non-emulsified QS sample. In addition, the emulsified samples showed an increase in the b^*-value, indicating a color shift toward yellow. For the SPI treatments, the addition of the emulsified feed to the extrusion process resulted in only modest changes in color values, significantly affecting only the a^*-values (Table 3). This indicates that the samples appeared less red when the SPI-stabilized emulsions were added to the liquid feed instead of bulk oil, which might be due to the scattering effects of the oil droplets. Still, the overall impact of the droplet size of the SPI-stabilized emulsions on the appearance of the HMMA was very small. This is in contrast to the study of Wang *et al.*,[20] in which a SPI-stabilized emulsified feed was also incorporated into an HMMA production process. From a comparison of photos, samples obtained in that study appeared much lighter compared to the HMMA treatments in the present study at similar oil concentrations. This might be related to a later injection point (4th barrel section in the study by Wang *et al.*[20]). Injection of the emulsion into the barrel section closer to the cooling die may have prevented excessive destabilization of the emulsion and thus more intact oil droplets may have been present. This could have increased light scattering which resulted in a brighter appearance (higher L^*-value). However, no color measurements were performed in this comparative study making it difficult to quantify the difference.

The color difference ΔE between all samples containing non-emulsified oil and the standard without oil was greater than 2.3, which is close to the threshold (2.5) of the JND (just-noticeable difference) rang in the CIELAB color space for the untrained observer.[46] While the value of the control with SPI showed only a minor difference to the control without the emulsifier (1.5), the control containing QS showed a distinct color difference to the control (4.0) and the standard (5.8). Because only minor changes in L^*-, a^*-, and b^*-values were seen for the emulsified treatments, the color differences ΔE to the standard were also relatively low. Since the samples with ΔE exceeding 2.5 occurred randomly among all emulsified treatments, no clear trend could be identified.

4. Conclusions

In summary, this study aimed to elucidate the different effects of adding bulk oil and emulsified oil feeds with different droplet sizes on an HMMA process and compare the product properties to the standard prepared with no oil addition. The results show that the emulsification – especially when using QS – lowered the die pressure and SME even more than bulk oil addition compared to the standard. However, this reduction did not reflect in the texture formation of the HMMA treatments as QS-stabilized emulsion samples were able to resemble both stress-based and elastic anisotropy indices of the standard. Therefore, the use of emulsified oil feeds with heat-stable surfactants can help to overcome the challenge in extrusion processing of extensive slip through bulk oil addition and thereby loss of anisotropic structure formation. The visual fibrousness was most pronounced for non-emulsified oil treatments due to intensified phase separation and reduced cross-linking between protein strings. Therefore, future studies should focus on two main aspects to advance the production of composite HMMA: (a) determine the impact of mechanical anisotropy and visual fibrousness on resemblance of

meat-like tissue; (b) reveal the lubricating effects of emulsified *vs.* bulk oils in such protein matrices at different oil concentrations by using heat-stable emulsifiers.

Data availability

The authors will provide data upon request.

Conflicts of interest

There are no conflicts to declare.

Acknowledgements

One of the authors (FS) acknowledges support from the Baden-Württemberg Program. The authors would like to thank Julian D. McClements for providing access to the CLSM and particle size measurement device as well as Roman Villiger from Three-Tec GmbH for the helpful discussion on the extrusion process.

References

1 GFI, *Pland Based State of the Industry Report 2022*, 2023.
2 D. J. McClements and L. Grossmann, *Compr. Rev. Food Sci. Food Saf.*, 2021, **20**, 1–52, DOI: **10.1111/1541-4337.12771**.
3 V. Bouvard, D. Loomis, K. Z. Guyton, Y. Grosse, F. E. Ghissassi, L. Benbrahim-Tallaa, N. Guha, H. Mattock and K. Straif, *Lancet Oncol.*, 2015, **16**, 1599–1600, DOI: **10.1016/S1470-2045(15)00444-1**.
4 J. De Boer, H. Schösler and H. Aiking, *Appetite*, 2017, **113**, 387–397, DOI: **10.1016/j.appet.2017.03.007**.
5 A. J. McAfee, E. M. McSorley, G. J. Cuskelly, B. W. Moss, J. M. W. Wallace, M. P. Bonham and A. M. Fearon, *Meat Sci.*, 2010, **84**, 1–13, DOI: **10.1016/j.meatsci.2009.08.029**.
6 J. Sabaté, K. Sranacharoenpong, H. Harwatt, M. Wien and S. Soret, *Public Health Nutr.*, 2015, **18**, 2067–2073, DOI: **10.1017/S1368980014002377**.
7 B. L. Dekkers, R. M. Boom and A. J. van der Goot, *Trends Food Sci. Technol.*, 2018, **81**, 25–36, DOI: **10.1016/j.tifs.2018.08.011**.
8 A. E. Lazou, *Crit. Rev. Food Sci. Nutr.*, 2022, 1–29, DOI: **10.1080/10408398.2022.2143474**.
9 D. J. McClements and L. Grossmann, in *Next-Generation Plant-Based Foods*, Springer International Publishing, Cham, 2022, pp. 89–153.
10 N. Köllmann, F. K. G. Schreuders, L. Zhang and A. J. van der Goot, *J. Food Eng.*, 2023, 111490, DOI: **10.1016/j.jfoodeng.2023.111490**.
11 J. L. Sandoval Murillo, R. Osen, S. Hiermaier and G. Ganzenmüller, *J. Food Eng.*, 2019, **242**, 8–20, DOI: **10.1016/j.jfoodeng.2018.08.009**.
12 M. P. Caporgno, L. Böcker, C. Müssner, E. Stirnemann, I. Haberkorn, H. Adelmann, S. Handschin, E. J. Windhab and A. Mathys, *Innovative Food Sci. Emerging Technol.*, 2020, **59**, 102275, DOI: **10.1016/j.ifset.2019.102275**.
13 C. Kendler, A. Duchardt, H. P. Karbstein and M. A. Emin, *Foods*, 2021, **10**, 697, DOI: **10.3390/foods10040697**.
14 D. Oppen, L. Grossmann and J. Weiss, *Crit. Rev. Food Sci. Nutr.*, 2022, 1–19, DOI: **10.1080/10408398.2022.2113365**.
15 C. Woern, A. G. Marangoni, J. Weiss and S. Barbut, *Food Res. Int.*, 2021, **147**, 110431, DOI: **10.1016/j.foodres.2021.110431**.
16 J. E. Elzerman, A. C. Hoek, M. A. J. S. Van Boekel and P. A. Luning, *Food Qual. Prefer.*, 2011, **22**, 233–240, DOI: **10.1016/j.foodqual.2010.10.006**.
17 V. Guyony, F. Fayolle and V. Jury, *Food Rev. Int.*, 2022, 1–26, DOI: **10.1080/87559129.2021.2023816**.
18 M. N. Riaz, in *Proteins in Food Processing*, Elsevier, 2004, pp. 517–558.
19 S. Gwiazda, A. Noguchi and K. Saio, *Food Struct.*, 1987, **6**, 57–61.
20 H. Wang, L. Zhang, T. P. Czaja, S. Bakalis, W. Zhang and R. Lametsch, *Food Res. Int.*, 2022, **158**, 111554, DOI: **10.1016/j.foodres.2022.111554**.
21 V. Zambrano, R. Bustos, Y. Arozarena and A. Mahn, *Foods*, 2023, **12**, 3869, DOI: **10.3390/foods12203869**.
22 Y. Yang, M. E. Leser, A. A. Sher and D. J. McClements, *Food Hydrocolloids*, 2013, **30**, 589–596, DOI: **10.1016/j.foodhyd.2012.08.008**.
23 K. Kohlgrüber and M. Bierdel, *Co-rotating Twin-Screw Extruders: Fundamentals, Technology, and Applications*, Carl Hanser Publishers; Hanser Gardner Publications, Munich, Germany, 2008.
24 G. A. Krintiras, J. Göbel, W. G. Bouwman, A. Jan Van Der Goot and G. D. Stefanidis, *Food Funct.*, 2014, **5**, 3233–3240, DOI: **10.1039/C4FO00537F**.
25 K. Sano, Y. Ishida and T. Aida, *Angew. Chem., Int. Ed.*, 2018, **57**, 2532–2543, DOI: **10.1002/anie.201708196**.
26 *Colorimetry: Understanding the CIE System*, ed. J. Schanda, Wiley, 1st edn, 2007.
27 A. R. Robertson, *Color Res. Appl.*, 1977, **2**, 7–11, DOI: **10.1002/j.1520-6378.1977.tb00104.x**.
28 D. J. McClements, *Food Emulsions: Principles, Practices, and Techniques*, 3rd edn, CRC Press, Florida, 2015.
29 D. J. McClements and L. Grossmann, in *Next-Generation Plant-Based Foods*, Springer International Publishing, Cham, 2022, pp. 23–88.
30 M. Suparno, K. D. Dolan, P. K. W. Ng and J. F. Steffe, *J. Food Process Eng.*, 2011, **34**, 961–982, DOI: **10.1111/j.1745-4530.2009.00381.x**.
31 P. Wittek, F. Ellwanger, H. P. Karbstein and M. A. Emin, *Foods*, 2021, **10**, 1753, DOI: **10.3390/foods10081753**.
32 R. Saha, R. V. S. Uppaluri and P. Tiwari, *J. Ind. Eng. Chem.*, 2018, **59**, 286–296, DOI: **10.1016/j.jiec.2017.10.034**.
33 F. L. Chen, Y. M. Wei and B. Zhang, *LWT–Food Sci. Technol.*, 2011, **44**, 957–962, DOI: **10.1016/j.lwt.2010.12.008**.
34 S. Mitra and S. R. Dungan, *J. Agric. Food Chem.*, 1997, **45**, 1587–1595, DOI: **10.1021/jf960349z**.
35 Y. Li, X. Liu, H. Liu and L. Zhu, *Food Hydrocolloids*, 2023, **136**, 108295, DOI: **10.1016/j.foodhyd.2022.108295**.
36 M. Keerati-u-rai and M. Corredig, *Food Hydrocolloids*, 2009, **23**, 2141–2148, DOI: **10.1016/j.foodhyd.2009.05.010**.
37 J. Ubbink and B. J. Muhialdin, *Phys. Fluids*, 2023, **35**, 087130, DOI: **10.1063/5.0161352**.

38 I. Capek, *Adv. Colloid Interface Sci.*, 2004, **107**, 125–155, DOI: 10.1016/S0001-8686(03)00115-5.
39 G. Palazolo, D. Sorgentini and J. Wagner, *Food Hydrocolloids*, 2005, **19**, 595–604, DOI: 10.1016/j.foodhyd.2004.10.022.
40 T. M. Bikbov, V. Y. Grinberg, H. Schmandke, T. S. Chaika, I. A. Vaintraub and V. B. Tolstoguzov, *Colloid Polym. Sci.*, 1981, **259**, 536–547, DOI: 10.1007/BF01397891.
41 J. Park, M. A. Plahar, Y. Hung, K. H. McWatters and J. Eun, *J. Sci. Food Agric.*, 2005, **85**, 1845–1851, DOI: 10.1002/jsfa.2192.
42 C. L. Reichert, H. Salminen and J. Weiss, *Annu. Rev. Food Sci. Technol.*, 2019, **10**, 43–73, DOI: 10.1146/annurev-food-032818-122010.
43 C. L. Reichert, H. Salminen, J. Utz, G. Badolato Bönisch, C. Schäfer and J. Weiss, *Colloid Interface Sci. Commun.*, 2017, **21**, 15–18, DOI: 10.1016/j.colcom.2017.10.003.
44 B. L. Dekkers, R. Hamoen, R. M. Boom and A. J. Van Der Goot, *J. Food Eng.*, 2018, **222**, 84–92, DOI: 10.1016/j.jfoodeng.2017.11.014.
45 S. Taghian Dinani, J. P. Van Der Harst, R. Boom and A. J. Van Der Goot, *Food Hydrocolloids*, 2023, **134**, 108059, DOI: 10.1016/j.foodhyd.2022.108059.
46 B. Hill, Th. Roger and F. W. Vorhagen, *ACM Trans. Graphics*, 1997, **16**, 109–154, DOI: 10.1145/248210.248212.